



# Clinical Drivers for Personalization of Transcranial Current Stimulation (tES 3.0)

# 24

Giulio Ruffini, Juilien Modolo, Roser Sanchez-Todo, Ricardo Salvador, and Emiliano Santarnecchi

## 24.1 Introduction

The brain is a complex, plastic, electrical *network* operating at multiple scales. There is a growing body of evidence suggesting that large-scale networks underlie both integration and differentiation processes that are fundamental for information processing. For instance, putatively simple cognitive tasks such as object recognition have been shown to involve networks that include the bilateral occipital, the left temporal, and the left/right frontal regions [1]. Neuropsychiatric disorders ultimately result from network dysfunctions that may arise from the abnormality in one or more isolated brain regions but produce alterations in larger brain networks (see [2–4]). Because of these observations, networks are natural targets of therapeutic interventions [5].

Interest in *neuromodulation* has increased in recent decades and it is now considered a promising tool for the management of conditions that range from psychiatric diseases to chronic neuropathic pain and epilepsy. Transcranial electrical current

---

G. Ruffini · R. Sanchez-Todo · R. Salvador  
Neuroelectronics Corporation, Cambridge, MA, USA  
e-mail: [giulio.ruffini@neuroelectronics.com](mailto:giulio.ruffini@neuroelectronics.com);  
[roser.sanchez@neuroelectronics.com](mailto:roser.sanchez@neuroelectronics.com); [ricardo.salvador@neuroelectronics.com](mailto:ricardo.salvador@neuroelectronics.com)

J. Modolo  
Univ Rennes, INSERM, LTSI—U1099, Rennes, France  
e-mail: [julien.modolo@inserm.fr](mailto:julien.modolo@inserm.fr)

E. Santarnecchi (✉)  
Berenson-Allen Center for Non-invasive Brain Stimulation,  
Beth Israel Deaconess Medical Center, Boston, MA, USA

Harvard Medical School, Boston, MA, USA  
e-mail: [esantarn@bidmc.harvard.edu](mailto:esantarn@bidmc.harvard.edu)

© Springer Nature Switzerland AG 2020  
B. Dell’Osso, G. Di Lorenzo (eds.), *Non Invasive Brain Stimulation in Psychiatry and Clinical Neurosciences*,  
[https://doi.org/10.1007/978-3-030-43356-7\\_24](https://doi.org/10.1007/978-3-030-43356-7_24)

stimulation (*tES*<sup>1</sup>) or transcranial current stimulation (*tCS*), as it is also known, is a safe [6], tolerable, noninvasive brain stimulation technique. Its origins follow the history of the discovery of electricity itself. Work in the twentieth century using low-intensity currents culminated in the investigation of weak direct and alternating currents by Nitsche and Paulus [7], who demonstrated that by applying a direct current through the scalp, the excitability of brain tissue can change up to 40%, as revealed by transcranial magnetic stimulation (TMS).

By passing electrical currents through the scalp and into the brain, *tES* generates *electric fields* that can alter brain function by coupling to neurons. A weak electric field can shift the neuronal membrane operating point, in a way that will make the cell more or less excitable, or, equivalently, more or less likely to fire given some inputs. This means that an electric field can immediately alter the way that the exposed part of the brain processes information, leading to longer-term changes through plasticity. Thus, by shifting the operating point of neurons, *tES* electric fields can affect the way parts of the brain participate in tasks (motor, cognitive, or others), and through *plasticity mechanisms*, contribute to its rewiring. *tES* comprises a number of *different techniques*: transcranial direct current stimulation (tDCS), alternating current stimulation (tACS), and random noise stimulation (tRNS) [8]. While other temporal waveforms are possible, the common elements of *tES* are the weak character of currents (typically below 2 mA) and spectral support below a few hundred Hertz (extremely low frequencies, <300 Hz). In tACS, the stimulation currents have a sinusoidal time dependence (as in AC current). Amplitude, frequency, and relative phases across stimulation electrodes can be controlled. tACS stimulation may provide a powerful way to couple to the oscillatory behavior of the brain, which is at present an active research field in basic and clinical neuroscience. In tRNS, a less explored *tES* modality, the stimulation current is varied randomly. Its main effects appear to be excitatory.

*tES* is similar, in terms of physical principles, to *transcranial magnetic stimulation (TMS)*, or electroconvulsive therapy (ECT), as all operate through the induction of electric fields in the brain. However, compared to TMS and ECT, in *tES* the generated electric fields are orders of magnitude weaker (see Figs. 24.1 and 24.2). *TMS* creates quite strong and brief electric field pulses that actually cause neuron firing (action potentials). A repetitive TMS (rTMS) session for depression delivers 3000 TMS pulses each ~0.2 ms wide, which sum to ~1 second of total effective stimulation (rounded, the precise number depends on pulse shape) with a peak field strength of ~150 V/m. Multiplying time of effective application and peak electric field gives a rough measure of dose of of 150 V·s/m that can be compared to other stimulation

---

<sup>1</sup>Abbreviations used: *ASL* arterial spin labeling, *BCM* Bienenstock, Cooper, and Munro plasticity theory, *CSF* cerebrospinal fluid, *ECT* electroconvulsive therapy, *EEG* electroencephalography, *EN* epileptogenic network, *fMRI* functional MRI, *GM* grey matter, *HBM* hybrid brain model, *MEG* magnetoencephalography, *MRI* magnetic resonance imaging, *NIRS* near-infrared spectroscopy, *NMM* neural mass model, *SEEG* stereographic EEG, *tACS* transcranial alternating current, *tDCS* transcranial direct current, *tCS* transcranial current stimulation, same as *tES* transcranial electrical stimulation, *tRNS* transcranial random noise stimulation, *STDP* Spike Timing Dependent Plasticity, *TMS* transcranial magnetic stimulation, *WM* white matter

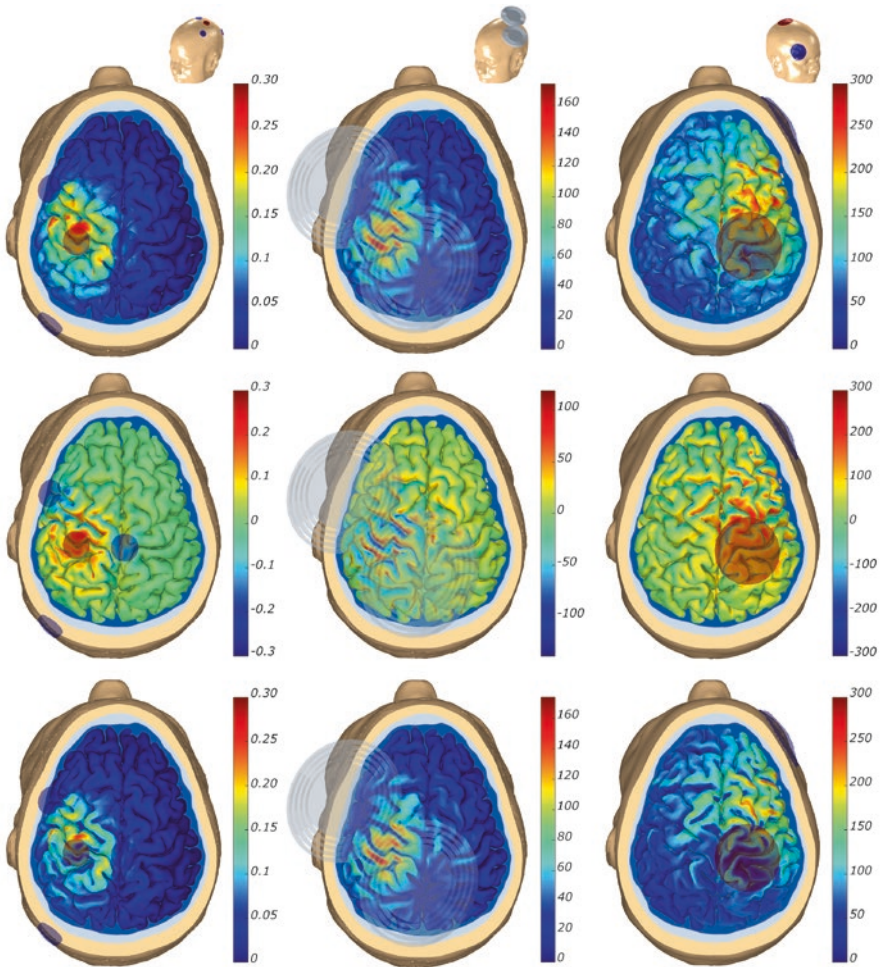


**Fig. 24.1** Electric field distribution in the cortical surface induced by tDCS (left column), TMS (central column), and ECT (right column). The top row shows the magnitude of the  $E$ -field, the middle row the normal component (positive/negative when the  $E$ -field is directed in/out of the cortical surface) and the bottom row the magnitude of the tangential component of the  $E$ -field. Typical electrodes/coils and stimulation intensities were used to calculate the  $E$ -field: multichannel montage with PiSTIM electrodes (1 cm radius, cylindrical Ag/AgCl electrodes) with a total injected current of 1.0 mA in the tDCS model; Magstim's 70 mm figure-8 coil at 67.7 A/ $\mu$ s for the TMS calculations (the value reported in the literature for the RMT using this coil, [9]); bipolar montage (frontoparietal right unilateral, FP-RUL configuration) with 5 cm diameter cylindrical electrodes and a 800 mA current in the ECT model. All  $E$ -field values are reported in V/m. The head model in which the simulations were run is common for all cases

techniques. *ECT* generates strong peak electric fields of about 400 V/m with current of  $\sim$ 800 mA [10] applied over timescales of about a few tenths of a second, with delivered charges of the order of a few hundred mC. *tES* induces weak electric fields that gently modify neuronal oscillations during relatively long times (20 minutes or

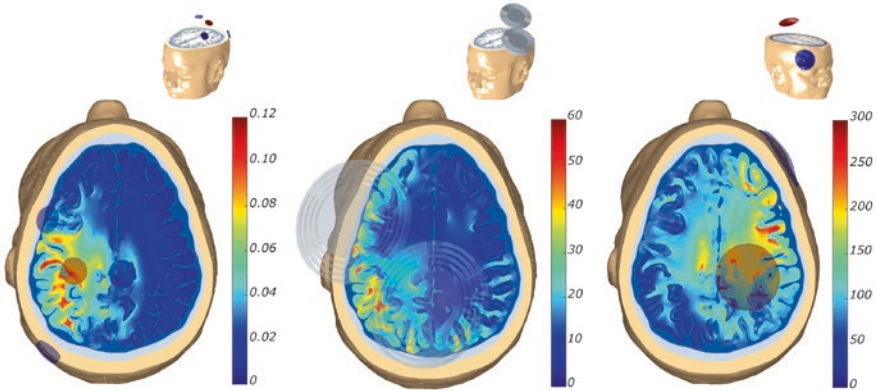


**Fig. 24.2** Magnitude of the electric field induced by tDCS (left column), TMS (central column), and ECT (right column) in an axial slice cutting through the GM and WM. The location of the slice with respect to the coil/electrodes is shown in the figures' insets. The parameters of the electrodes and coil are the same as described in Fig. 24.1. All  $E$ -field values are reported in V/m. The head model in which the simulations were run is common for all cases

**Table 24.1** A comparison of different stimulation dose metrics based on peak field and time of application – but not area – using representative numbers in each case (for ECT and rTMS as used in depression)

Metric (units)	tES	rTMS	ECT
Peak field in cortex, $E_{\text{peak}}$ (V/m)	0.5	150	400
Injected current (mA)	1	-	800
Summed pulse Duration, $T$ (s)	1200	1	0.2
Charge delivered, $Q$ (mC)	1200	-	160
Amplitude-duration, $E_{\text{peak}} \times T$ (V s/m)	600	150	80

more), with  $\sim 0.5$  V/m peak field, or a dose of 600 V s/m and delivered charges of the order of 1200 mC [11]. In all cases, multiple sessions are employed for therapeutic results. See Table 24.1 for a comparison of dosing between these techniques. To note that, since the therapeutic mechanisms of action are not well understood for any of them, our dosing comparison remains indicative.

Traditionally, tES has been applied using two large sponge electrodes on the scalp. However, newer systems use several small, EEG-like electrodes. Aided by realistic *modeling*, *multielectrode tES* can be used to produce controlled, precise electric fields in the brain, resulting in more specific electric field distributions and less variable effects [8, 12, 13]. tES is naturally combined with the measurement of *EEG* since both technologies rely on the electrical nature of the human brain. EEG can be used to study changes induced by tES, comparing the effects across groups or pre- and poststimulation. Similarly, tES is also often combined with fMRI, ASL, and NIRS, for example, for the study of brain networks pre-, during- and post-stimulation.

*Research* with tES includes basic neurophysiology and cognitive neuroscience. Basic research with tES (and its combination with other techniques) has the goal of deciphering the way the human brain works. By altering the operating points of neural networks, information can be gathered on fundamental mechanisms. This provides the means for realizing causal studies rather than correlation-based ones. *Clinical applications* of tES have been studied for almost two decades. The most mature ones are in fibromyalgia, major depression without drug resistance and in addictions/cravings (with probable efficacy, Level B evidence [14]), but many others are being developed, including epilepsy, chronic neuropathic pain, tinnitus, major depression with drug resistance, brain cancer, and cognitive remediation in neurodegeneration. Clinical applications of tES rely, mostly, on its plastic effects (those that remain after treatment is over). Under the hypothesis that brain function depends on its connectivity, neuromodulation aims to rewire the brain to achieve therapeutic effects.

Today, tES montages are *optimized* on the assumption that the effects can be directly quantified from the measurement of the electric field on the cortex, as we discuss more in-depth below. However, we know that such “passive electrical” physical models cannot fully describe the complex physiological phenomena that underlie brain function and stimulation effects (the physics of *life*). As neuroscience moves from a correlation-based science to a model-driven one, *computational models of the brain* (physics of electric fields and of their interaction with complex, active neuronal networks) will play a key role in the development of novel mechanistic understanding and computational optimization strategies for brain stimulation.

In this chapter, we will focus on the treatment of *disorders with oscillatory signatures*. On the one hand, *epilepsy* is characterized by hypersynchronous oscillations stemming from the hyperactivation of one or more foci. Drug-resistant epilepsies represent not only a considerable challenge for the health care system but also a tremendous burden at the individual, family, and community levels. They are characterized by an epileptogenic network (EN) interconnecting distant brain areas located in one of the two hemispheres. There is a large body of evidence suggesting that patient-specific ENs [15] are responsible for the generation and spread of seizures through synchronization processes that interconnect neuronal assemblies with altered excitability [16]. Such networks are the potential targets for therapy. *Depression* manifests alterations in the alpha (~10 Hz) [17–19] and gamma frequency EEG bands [20]. Similarly, patients with *PTSD* also display alterations in the alpha and gamma band, characterized by intrinsic sensory hyperactivity (i.e., suppressed posterior alpha power, localized to the visual cortex—cuneus and precuneus) and increased gamma activity in the prefrontal lobe as compared to patients with generalized anxiety disorder and healthy control subjects [21]. Finally, patients with *schizophrenia* [22, 23] and *autism spectrum disorder (ASD)* [24, 25] as well as neurodegenerative disorders such as *Alzheimer’s disease (AD)* and *frontotemporal dementia (FTD)* [26], all present disturbances in the gamma frequency band, with additional involvement of slower frequencies (e.g., theta) and their coupling. These disturbances often manifest themselves in different systems or networks and arise from different neuropathological substrates. Models able to incorporate the

complex physiology of the healthy brain—and its variation when pathology arises—are needed to develop disease-modifying therapies.

We discuss below how hybrid models can be used to represent such pathologies to develop *in silico* treatment optimization strategies through the combination of tES and drugs. When informed by the relevant patient data, such models can, for instance, define individual stimulation frequency in tACS, taking into account (1) individual brain anatomy and cortical folding, (2) the location of cortical and subcortical oscillators, (3) cortical columnar organization and the corresponding layer-specific generators for activity in different frequency bands, (4) layer-to-layer interplay supporting cross-frequency coupling (e.g., theta-gamma coupling), (5) distribution/location of inhibitory and excitatory neuronal populations (e.g., GABAergic interneurons targeted via gamma-tACS in the case of AD and Schizophrenia), and many other features currently not accessible via canonical modeling work. Here, we comment on some of the efforts currently being made in this direction, supporting the adoption of hybrid models by the clinical community.

As we will see, the use of HBMs enables what may be called *tES 3.0*, where tES 1.0 refers to the early use of sponges, with bipolar montages and targets defined on electrode space, and tES 2.0 to the current use of multielectrode systems with targets defined by the electrical field on the cortex [27]. tES 3.0 is the unfolding vision of EEG-guided multielectrode systems with personalized hybrid-model-driven targeting and optimization.

---

## 24.2 Realistic Physical Modeling of Passive Tissues

The electric field (abbreviated as *E*-field) induced in the brain by tES is the mechanistic link to the concurrent effects of stimulation [8]. Although some *in vivo* techniques are available to measure the *E*-field, they either require invasive methods [28, 29] or rely on complex setups, which currently cannot be implemented in any practical manner [30, 31]. The only method currently available to predict the *E*-field distribution in the brain with a high spatial resolution is numerical modeling of Maxwell's equations in conductive media. Modeling approaches for tES have matured over the last few years, now offering the possibility of generating subject-specific models of the distribution of the *E*-field in the brain for any montage [13]. These models can also be combined with optimization algorithms, to guide montage design in order to target specific regions or networks more efficiently.

The distribution of the *E*-field in the head is governed by well-known equations that apply to electrostatic phenomena: the *E*-field (in units of volts per meter, V/m) can be obtained by taking the gradient of the electrostatic potential ( $\Phi$  in units of volts, V), which obeys Laplace's equation [32]. These equations can be solved analytically for simple head geometries, like concentric spheres [32], but not for more complex shapes. For the latter, numerical techniques such as the finite element (FE) method—a method that is commonly used in tES *E*-field calculations [13, 33]—need to be employed.

Different pipelines are available to generate head models and obtain the solution with FE analysis [13, 34, 35], but they all follow essentially the same basic steps (see Fig. 24.3). The first step is creating a realistic geometric representation of the head tissues. This is usually done by relying on structural MRIs of the subjects, which are then segmented into the most important tissues (Fig. 24.3a): scalp, skull (sometimes with representations of air sinuses and separation between spongy and compact bone, [36]), cerebrospinal fluid (CSF, including the ventricles), gray matter (GM), and white matter (WM). Most pipelines rely on at least a T1-weighted MRI, which should not have any type of crop and offer enough neck coverage to guarantee accurate calculations for lower electrode positions [37]. Guidelines for optimizing the MRI sequences for segmentation purposes are available and it is crucial to follow them, as they minimize misclassifications of tissues during segmentation, which can impact  $E$ -field predictions [38]. These segmented tissue masks are then used to create triangulated surfaces of the different tissues. The latter renders the tissue interfaces as smooth, which is realistic from an anatomical perspective [39]. In the FE method, this geometry is then further discretized into smaller shapes called finite elements (usually tetrahedra) comprising the finite element mesh. At this stage, realistic representations of the electrodes are also added to the head model [40] (Fig. 24.3a). The FE method calculates  $\Phi$  within each finite element based on the values at the vertices of the finite elements (nodes of the mesh). The  $E$ -field can then be derived from the gradient of  $\Phi$ . This calculation requires knowledge about the currents in each electrode, as well as the electrical properties of the tissues (Fig. 24.3b). Biological tissues in the low-frequency range (i.e., below 1 kHz) can be represented as linear (ohmic) materials characterized by their electrical conductivity ( $\sigma$  in Siemens per meter, S/m). To date, there is still a wide range of electrical conductivity values reported in literature [41], and their estimation is an active area of research. One important property of the linear nature of biological tissues is that no phase differences arise between the waveform of the injected scalp current (in the case of tACS and tRNS) and that of the  $E$ -field in the tissues. This notion has been confirmed in *in-vivo* recordings [28]. Certain tissues, like white matter, have anisotropic conductivity profiles due to

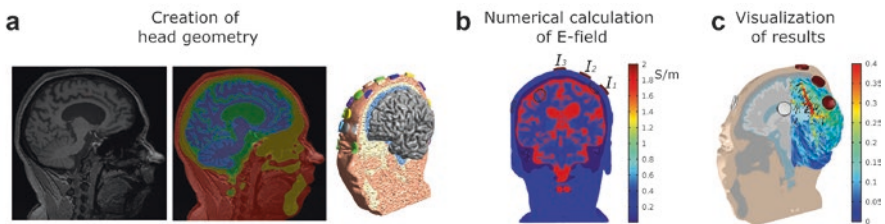


**Fig. 24.3** Typical steps involved in the creation of a head model for tES calculations. (a) Creation of the head model geometry from the anatomical data (T1w-MRI). (b) Numerical calculations of the  $E$ -field, which requires the specification of the electrical conductivities of each tissue (in units of S/m) and the currents of the electrodes. (c) Visualization of the  $E$ -field distribution in both the cortical surface (the magnitude of the  $E$ -field is shown in the figure, in V/m) and as a vector plot in a coronal slice through the WM and GM. Anodes are shown in red and cathodes in blue

constraints imposed by the alignment of fibers in charge flow in the brain [42]. This can also be included in the model, provided that diffusion-weighted MRIs are available for the subject being modeled [43].

The results of these calculations can be visualized as maps of the spatial distribution of the  $E$ -field displayed on the cortical surface (see Fig. 24.3c). Since the  $E$ -field is a vector, either the magnitude or a component of the field along a specific direction is normally displayed. Regarding the  $E$ -field components, most published studies focus on the component normal to the cortical surface ( $E_n$ ), which is thought to be the most determinant one to predict the polarization of pyramidal cells, which are aligned perpendicularly to the cortical surface [13, 27, 44]. These field values can also be averaged over cortical patches. Since it is likely that many neurons are affected by the  $E$ -field distribution of tES, these surface averaged values may be more appropriate to quantify the effects of a specific montage. In some studies, current density values ( $J$ , in units of Ampères per meter squared,  $A/m^2$ ) are presented, instead of the electric field [45]. This is another vector which, for isotropic tissues, is defined as the product of the electrical conductivity by the electric field vector. The range of values of  $J$  (or  $E$ ) is uncorrelated with the ratio of injected current by the electrode surface area, which is also mistakenly referred to as current density [46].

Computational head models have been used to study the basic properties of the  $E$ -field distribution in tES [12, 47], alternative electrode designs [48], or the influence of head lesions in the  $E$ -field distribution [49, 50]. These studies usually model the  $E$ -field distribution induced by specific montages used in trials in a retrospective manner. In recent years, however, models have also been combined with optimization algorithms to guide montage design [27, 51]. These optimization approaches take as input a target region in which a target  $E$ -field value is specified. The optimization algorithm then determines the montage, involving a pool of many electrodes in predefined positions (like the ones of the 10–10 EEG system, [52]) that better approximates the target  $E$ -field distribution. These optimization algorithms are typically combined with multichannel montages containing many small electrodes to generate more controllable  $E$ -field distributions [12, 47]. The optimization procedure can be conducted in a personalized way, using the computational head models created for each subject in the study. This is particularly important given the considerable intersubject variability in the  $E$ -field distribution due to anatomical differences [53]. Optimization-based montage design is ideally suited to target single ROIs as well as distributed brain networks, with the target maps being generated from the functional data, such as resting-state fMRI networks or the EEG data [54].

---

### 24.3 Physiological tES Models Across Scales

Since tES, depending on the montage used, can induce an electric field in the brain that can span across several brain regions, it is an absolute requirement to evaluate the effects of this electric field on neural elements. One major challenge is to understand and integrate how tES-induced electric field interacts with brain tissue at different spatial scales, from the single neuron or synapse level, to the large-scale



circuit level. Progress on that issue is especially important since understanding the fundamental mechanisms of tES might involve identifying the repercussions from the effects at one level (cellular) to the other (network). A related issue is understanding how an electric field of low magnitude (on the order of 1 V/m) can modulate brain tissue activity despite not being able to induce spiking (see [55] for a review). In order to understand how modulation of activity at the cellular level induces deregulations of oscillatory activity at the network level, which are associated with some neurological disorders, these issues need to be addressed.

At the single-cell level, it has been shown that the tES-induced electric field depolarizes the neuron membrane by approximately 0.2 mV per V/m of the *in situ* electric field [56]. Assuming a maximal value of an *in situ* electric field of 1 V/m, this implies that the membrane of neurons is depolarized by 0.2 mV, which is significantly lower than the depolarization required to induce spiking (on the order of 20 mV). These weak membrane perturbations may be seen to affect the function of dendrites, soma, axon hillock, and axon terminals in different ways. For example, modulation of cell firing patterns will be affected by polarization at the soma and axon hillock, while at axon terminals synaptic release may be affected. A few modeling studies have proposed that such global, weak polarization changes can impact spike timing and phase synchronization in local networks through nonlinear network-amplification effects [57]. Those cellular-scale results have direct implications to understand tES effects: spike timing is indeed crucial in the induction of synaptic plasticity changes, for example, through the Spike Timing Dependent Plasticity (STDP) rule [58]. It has been suggested that changes in spike timing of a few milliseconds, accumulated over several minutes, might induce gradual changes in synaptic weights due to the properties and asymmetry of the STDP rule, in line with the reported lasting effects of tES [59]. Furthermore, phase synchronization of firing in networks is a more subtle, but important effect, since it may explain changes in the amplitude of spontaneous, endogenous oscillations following tES [60]. Increasing/decreasing the phase synchronization of spiking from numerous neurons would result in an increase/decrease of the endogenous oscillation by modulation of coherence. Interestingly, support for this idea has emerged from experimental recordings in animals and humans [61–63].

A few studies have also investigated the brain-scale effects of tES. For example, a modeling study investigating the effects of alpha-frequency tES on simulated whole-brain activity and associated scalp EEG [64], pointed at a maximal effect of tES when the stimulation frequency was the same as the endogenous oscillation (alpha frequency), with an effect rapidly fading when the difference between the endogenous and stimulation frequencies increased. Therefore, one challenge and opportunity of tES seems that it can only modulate endogenous oscillations (and not induce *de novo* activity, since tES cannot induce spiking), possibly by matching the stimulation frequency close to the endogenous frequency and entraining activity. This could greatly improve the design of tES by targeting specific rhythms associated with the desired function. Overall, it appears that candidate mechanisms of tES have been identified at several scales, which could explain at least partly the reported effects in animals and humans. However, a unified model of the tES mechanism is

still lacking, a major challenge that could be addressed through the use of hybrid brain models (HBMs), which are reviewed in the next section.

---

## 24.4 The Architecture of HBMs

Today, model-driven optimization for multichannel transcranial stimulation is based on the physical features of the subject's brain, such as head geometry (extracted from MRI images) and tissue conductivities, as mentioned in previous sections. Nevertheless, there is a clear need to expand the horizon of optimization to more sophisticated models that also represent physiological information of the subject. In this section, we will explain how to combine the physical and physiological data of the individual brain in order to create a personalized computational model and design more refined personalized optimization strategies—in other words, how to design a Hybrid Brain Model.

In the framework where the brain is represented as a network, coupled mathematical differential equations (either ordinary or partial) can be used to describe the spatiotemporal dynamics of brain activity and traveling waves [65], at the level of one node or of larger-scale networks, corresponding to multiple coupled nodes. Traditionally, two main classes of models have been used to derive these differential equations. On the one hand, spiking neuron models such as the Hodgkin-Huxley model [66] describe the detailed dynamics of individual neurons. On the other hand, neural mass models (NMMs) such as the Wilson-Cowan model [67] provide effective theories of neural systems. The former, a more detailed class of models, is appropriate for representing single-cell recordings in animals or brain slices, but their state variables do not directly—at least without very large computational demands—capture the functional activity recorded with macroscopic level techniques such as Electroencephalography (EEG), Magnetoencephalography (MEG) or mesoscopic Local Field Potential (LFP) measurements. In contrast, NMMs are more useful for modeling brain activity at larger spatial and temporal scales, since they describe the mean activity of whole neural populations. While providing a lower level of detail, their parameters emerge from microscopically measurable quantities, such as dendritic time constants and mean excitatory/inhibitory postsynaptic potentials, and they are able to represent the physiology of the brain as observed by macroscale measurements.

An *HBM* is essentially a *physically-situated network* in which NMMs constitute the *nodes*. Depending on the data available or the scale of the model, network nodes can represent either single columns, cortical patches, or whole-brain areas (see the extended review by Breakspear [68] for a detailed discussion on the choices of dynamical equations). Accordingly, network edges or *links* are needed to describe appropriately the links between nodes. For example, to model whole-brain dynamics [67], coupling strength is often defined in proportion to the number of white matter tracts (structural connectivity) between brain areas using the well-known human connectome [69]. However, functional or effective connectivity can also be used to define these links [70–72].

As mentioned above, one of the advantages of HBMs is that they can make a connection with macroscopic measurements. For example, the activity of NMM nodes in the HBM can be used to simulate cortical dipole source activity field  $J(x,t)$ , where  $x$  denotes a cortical source location and  $t$ , time. Since the NMM network is embedded in a known physical matrix that describes its electrical characteristics, the dipole field can be mapped to *EEG* electrode space activity using the “lead field” forward map [64, 73, 74]. Similar methods can, in principle, be used to model *MEG* or *fMRI*. The effects of *tES* can be represented on the grounds of known or hypothesized interaction mechanisms. The *lambda-E* model [8, 27, 64, 75, 76], for example, posits that the main effect of *tES* is to modulate the polarization of pyramidal cells in a manner proportional to the electric field component parallel to the cells’ main axis (from apex to soma). Similarly, TMS’s effects are assumed to be mostly due to electric field magnitude and are known to cause neuron spiking from strong depolarization. All these effects are readily represented in an NMM and, in consequence, in a HBM. All that is required is to calculate the electric field on the realistic head model. The effects of *drugs* on neurons can also be represented if their physiological mechanisms are known [77, 78]. For example, in the case of antiepileptic drugs [79], some molecules decrease the excitability of pyramidal cells (e.g., voltage-gated sodium channel blockers such as carbamazepine, or voltage-gated calcium channel blocker such as Zonisamide) or modulate cellular connectivity (GABA-A enhancers such as Clobazam, or NMDA antagonists such as Felbamate). HBMs can also represent network *plasticity* and the plastic impact of *tES* [76]. Plastic phenomena can be adapted in these models by encoding known Hebbian mechanisms (“cells that fire together, wire together, cells that fire apart, wire apart”) such as BCM or Oja’s rules [80]. To first order, their implementation will include the change connectivity constants within the NMM nodes (local scale) as a function of the history of the activity of the model, across them (large network or structural scale), or both. Other parameters can be modified as well.

The *personalization* of a model starts by using individual MRI (anatomy) and DTI (connectivity) data (see Fig. 24.4). DTI and MRI are used to connect the NMMs, to have information about physiological connections, anatomy, and physical distance between brain regions, and to represent macroscale electrical phenomena. Bansal et al. [81] and Aerts et al. [82] review recent research on personalized whole-brain models. The former is related to the study of structure-function relationship in human brains, while the latter focuses on the impact of network lesions. The majority of the studies cited in these reviews only use the structural connectivity brain data derived from DTI to personalize whole-brain models. Moreover, most of the models in those studies are based on static model parameters, failing to reproduce some meaningful features on individual brain dynamics.

Crucially, since they can be used to simulate and predict measurements, in addition to the structural data, HBMs can ingest physiological measurements (e.g., EEG, SEEG, fMRI, and EN)—much as weather or climate models do. Physiological data are used to adjust the desired parameters of the model. The most currently used approaches fit the data in the form of Functional Connectivity (FC) profile between regions [73, 83], but others can be used. That is, parameters are adjusted so that

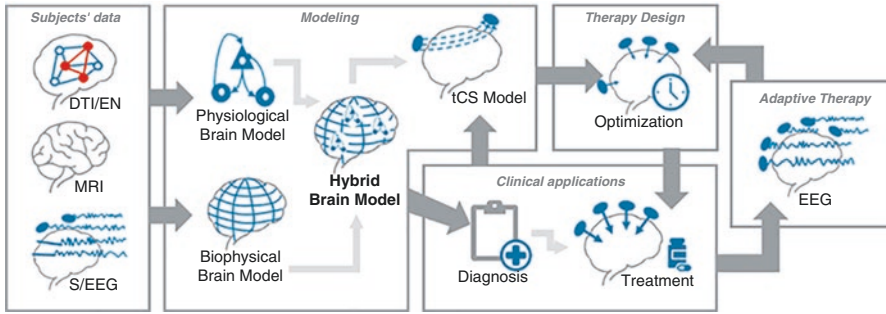


**Fig. 24.4** Workflow for the creation of hybrid-model-driven tES optimization. The DTI and anatomical MRI data are combined to create a finite element biophysical model (FEM), which is then personalized using EEG and/or SEEG (S/EEG), EN, and other data to reflect both biophysical and physiologic characteristics—from excitation/inhibition balance to plastic potential (long-term effect physiological model). The personalized hybrid brain model can be used to generate EEG and to simulate the effects of brain stimulation. As a result, personalized diagnosis and treatment can be applied, such as optimized stimulation protocols. Since tES protocols are typically multisession, the EEG data collected over time (e.g., at patient’s home, using telemedical solutions) can be used to refine models and adapt the stimulation protocols (target map, dosing)

model generated FC across cortical regions matches that inferred from dense EEG measurements (after cortical mapping, see [73] and [5], for example). More specifically, the EEG data can be processed to extract functional connectivity from the power envelope in a given frequency band [74, 75], which can then be matched with NMM activity at each parcel [73].

## 24.5 Tailoring and Adapting Interventions

As we have seen, today, tES montages are optimized on the assumption that the effects can be directly quantified from the knowledge of the electric field on the cortex. For example, a neurologist may want to reduce the excitability of a brain region under the assumption that this will lead to beneficial plastic network effects. In order to do so, it suffices to demand for the electric field to be adequately intense and properly oriented with respect to the cortical surface (pointing out, to be specific). However, such an approach ignores the complexity of nonlinear network interactions associated with brain physiology. *Specifying a target function* in such a manner is equivalent to making crucial assumptions about mechanisms and cascade effects at the system level. A more natural way of doing so would be to simply state “I want to disconnect this node from this network” in an epileptic patient, for example, or “I would like to increase gamma activity in these regions” (in AD, for example), and let a physiologically grounded algorithm take care of the analysis and solution. This is the vision of hybrid modeling: helping the clinician focus on the causes of the disease, presumably at the connectivity (micro or macro) level, and finding a computational grounded solution. Moreover, accurate modeling combined

with regular patient monitoring, big data, and artificial intelligence approaches could pave the way for “adaptive therapeutics”, where the individual patient data are used to refine tES parameters on a daily/weekly/monthly basis (see Fig. 24.4). Future implementations of hybrid models may allow the prediction of structural/functional brain changes induced by a given therapy, and, combined with the incoming patient data, “correct” the therapeutic trajectory accordingly.

From the large body of evidence that is accumulating regarding the effects of tES on brain activity, some possibilities of *future developments of this technique are emerging*. Since dynamic tES appears to mediate its effects mainly on endogenous rhythms, by matching the stimulation frequency with those endogenous rhythms, one possibility would be to characterize the function to be targeted in terms of associated neural oscillations. This would provide the temporal characteristics of the stimulation to be applied. To go further, mapping the functional network associated with the targeted function, and deriving corresponding multi-site tES montages through hybrid models, would provide the spatial characteristics of the stimulation protocol. By combining both types of information, tES could provide a spatiotemporal modulation of function-specific neuronal activity. That being said, what are the neurological disorders that could benefit the most from this “tES 3.0” strategy? First of all, conditions where the pattern of altered metabolic/functional activity is widespread—such as dementias in primis. In the case of Alzheimer’s disease, multi-site tES could be optimized to tackle hypometabolic regions [84], areas affected by amyloid and tau deposition [85], as well as nodes of mostly affected brain functional networks (e.g., default mode network) [86]. Moreover, recent evidence points toward specific alterations of high-frequency activity within the gamma band, involving dysfunction of GABAergic parvalbumin (PV+) inhibitory interneurons. This specific neurophysiological substrate requires, among other aspects, the optimization of stimulation solutions able to entrain gamma activity, and potentially do so by leveraging cross-frequency coupling dynamics [87], or via precise modeling of the interaction between PV+ cell(s) and pyramidal cells (PV+ ↔ PV+ inhibition circuit, PV+ ↔ pyramidal cell circuit). A hybrid model accounting for such circuitry could suggest different simulation solutions based on the proportion of residual interneurons and pyramidal cells, which might differ across regions (due to protein deposit and atrophy) and disease state.

Differently, psychiatric conditions not involving neurodegeneration tend to present a more local pattern of alteration, such as in the case of subgenual and prefrontal lobe changes in depression and cerebellar-prefrontal changes in schizophrenia. However, even though alterations might be more focal, other disease-specific factors come into place and make novel tES solutions equally needed. For instance, differential alterations of prefrontal GABA-A and GABA-B circuitry have been documented in schizophrenia, suggesting future therapeutic interventions to focus more on modulation of GABA-B dynamics for optimal cognitive remediation [88]. While such neurotransmitter-level targeted modulation is more intuitive for drug-based interventions, hybrid tES models accounting for intracolumnar dynamics could eventually identify cell-class specific targets and the corresponding optimal therapies.

## 24.6 Conclusions

By using hybrid models to represent brain activity and the impact of tES, better optimization algorithms can be developed. This methodology is widely applicable beyond tES to other brain stimulation modalities. By forcing the field to quantify mechanisms and etiology in computational models, advanced algorithms can provide novel and powerful solutions. At the same time, technological advances provide more tolerable and flexible experimental protocols. Already today, hybrid, wireless tES/EEG systems allow for the recording of EEG signals and stimulation using the same system and the same electrodes. Both for basic and clinical research applications, tES studies typically involve multiple stimulation sessions, because the effects of tES are cumulative. For this reason, the field benefits from the existence of controlled and safe home deployment solutions, allowing subjects to participate in studies without the need to visit the research lab or hospital on multiple occasions. The same solutions, collecting EEG and allowing for remote protocol modifications, will eventually provide the means for adaptive interventions in telemedicine.

---

## References

1. Price CJ, Moore CJ, Humphreys GW, Frackowiak RSJ, Friston KJ. The neural regions sustaining object recognition and naming. *Proc R Soc Lond Ser B Biol Sci.* 1996;263(1376):1501–7.
2. Fox MD, Halko MA, Eldaief MC, Pascual-Leone A. Measuring and manipulating brain connectivity with resting state functional connectivity magnetic resonance imaging (fcMRI) and transcranial magnetic stimulation (TMS). *Neuroimage.* 2012;62(4):2232–43.
3. Fox MD, Buckner RL, White MP, Greicius MD, Pascual-Leone A. Efficacy of transcranial magnetic stimulation targets for depression is related to intrinsic functional connectivity with the subgenual cingulate. *Biol Psychiatry.* 2012;72:595–603.
4. Fornito A, Zalesky A, Breakspear M. The connectomics of brain disorders. *Nat Rev Neurosci.* 2015;16(3):159–72.
5. Ruffini G, Wendling F, Sanchez-Todo R, Santarnecchi E. Targeting brain networks with multichannel transcranial current stimulation (tCS). *Curr Opin in Biomed Eng.* 2018;8:70–7.
6. Antal A, Alekseichuk I, Bikson M, Brockmüller J, Brunoni AR, Chen R, et al. Low intensity transcranial electric stimulation: safety, ethical, legal regulatory and application guidelines. *Clin Neurophysiol.* 2017;128(9):1774–809.
7. Nitsche MA, Paulus W. Excitability changes induced in the human motor cortex by weak transcranial direct current stimulation. *J Physiol.* 2000;527(Pt 3):633–9.
8. Ruffini G, Wendling F, Merlet I, Molae-Ardekani B, Mekkonen A, Salvador R, et al. Transcranial current brain stimulation (tCS): models and technologies. *IEEE Trans Neural Syst Rehabil Eng.* 2013;21(3):333–45.
9. Kammer T, Beck S, Thielscher A, Laubis-Herrmann U, Topka H. Motor thresholds in humans: a transcranial magnetic stimulation study comparing different pulse waveforms, current directions and stimulator types. *Clin Neurophysiol.* 2001;112:250–8.
10. Peterchev AV, Rosa MA, Deng Z-D, Prudic J, Lisanby SH. ECT Stimulus Parameters: Rethinking Dosage. *J ECT.* 2010 Sep;26(3):159–74.
11. Peterchev AV, Wagner TA, Miranda PC, Nitsche MA, Paulus W, Lisanby SH, et al. Fundamentals of Transcranial Electric and Magnetic Stimulation Dose: Definition, Selection, and Reporting Practices. *Brain Stimul.* 2012 Oct;5(4):435–53.

12. Miranda PC, Mekonnen A, Salvador R, Ruffini G. The electric field in the cortex during transcranial current stimulation. *Neuroimage*. 2013;70:45–58.
13. Miranda PC, Mekonnen A, Salvador R, Ruffini G. The electric field in the cortex during transcranial current stimulation. *Neuroimage*. 2013;70:45–58.
14. Lefaucheur J-P, Antal A, Ayache SS, Benninger DH, Brunelin J, Cogiamanian F, et al. Evidence-based guidelines on the therapeutic use of transcranial direct current stimulation (tDCS). *Clin Neurophysiol*. 2017 Jan;128(1):56–92.
15. Bartolomei F, Lagarde S, Wendling F, McGonigal A, Jirsa V, Guye M, et al. Defining epileptogenic networks: contribution of SEEG and signal analysis. *Epilepsia*. 2017;58(7):1131–47.
16. Wendling F, Bartolomei F, Mina F, Huneau C, Benquet P. Interictal spikes, fast ripples and seizures in partial epilepsies—combining multi-level computational models with experimental data. *Eur J Neurosci*. 2012;36(2):2164–77.
17. Iosifescu DV. Electroencephalography-derived biomarkers of antidepressant response. *Harv Rev Psychiatry*. 2011;19(3):144–54.
18. Nystrom C, Matousek M, Hallstrom T. Relationships between EEG and clinical characteristics in major depressive disorder. *Acta Psychiatr Scand*. 1986;73(4):390–4.
19. Baskaran A, Milev R, McIntyre RS. The neurobiology of the EEG biomarker as a predictor of treatment response in depression. *Neuropharmacology*. 2012;63(4):507–13.
20. Fitzgerald PJ, Watson BO. Gamma oscillations as a biomarker for major depression: an emerging topic. *Transl Psychiatry*. 2018;8(1):177.
21. Clancy K, Ding M, Bernat E, Schmidt NB, Li W. Restless ‘rest’: intrinsic sensory hyperactivity and disinhibition in post-traumatic stress disorder. *Brain*. 2017;140(7):2041–50.
22. Kirihaara K, Rissling AJ, Swerdlow NR, Braff DL, Light GA. Hierarchical organization of gamma and theta oscillatory dynamics in schizophrenia. *Biol Psychiatry*. 2012;71(10):873–80.
23. Senkowski D, Gallinat J. Dysfunctional prefrontal gamma-band oscillations reflect working memory and other cognitive deficits in schizophrenia. *Biol Psychiatry*. 2015;77:1010–9.
24. van Diessen E, Senders J, Jansen FE, Boersma M, Bruining H. Increased power of resting-state gamma oscillations in autism spectrum disorder detected by routine electroencephalography. *Eur Arch Psychiatry Clin Neurosci*. 2015;265(6):537–40.
25. Sun L, Grützner C, Bölte S, Wibrall M, Tozman T, Schlitt S, et al. Impaired gamma-band activity during perceptual organization in adults with autism spectrum disorders: evidence for dysfunctional network activity in frontal-posterior cortices. *J Neurosci*. 2012;32(28):9563–73.
26. Palop JJ, Mucke L. Network abnormalities and interneuron dysfunction in Alzheimer disease. *Nat Rev Neurosci*. 2016;17(12):777–92.
27. Ruffini G, Fox MD, Ripolles O, Miranda PC, Pascual-Leone A. Optimization of multifocal transcranial current stimulation for weighted cortical pattern targeting from realistic modeling of electric fields. *Neuroimage*. 2014;89:216–25.
28. Opitz A, Falchier A, Yan CG, Yeagle EM, Linn GS, Megevand P, et al. Spatiotemporal structure of intracranial electric fields induced by transcranial electric stimulation in humans and nonhuman primates. *Sci Rep*. 2016;6:31236.
29. Huang Y, Liu AA, Lafon B, Friedman D, Dayan M, Wang X, et al. Measurements and models of electric fields in the in vivo human brain during transcranial electric stimulation. *eLife*. 2017;6:e18834.
30. Göksu C, Hanson LG, Siebner HR, Ehses P, Scheffler K, Thielscher A. Human in-vivo brain magnetic resonance current density imaging (MRCDI). *Neuroimage*. 2018;171:26–39.
31. Kasinadhuni AK, Indahlastari A, Chauhan M, Schär M, Mareci TH, Sadleir RJ. Imaging of current flow in the human head during transcranial electrical therapy. *Brain Stimul*. 2017;10(4):764–72.
32. Rush S, Driscoll DA. EEG electrode sensitivity - an application of reciprocity. *IEEE Trans Biomed Eng*. 1969;16:15.
33. Johnson CR. Computational and numerical methods for bioelectric field problems. *Crit Rev Biomed Eng*. 1997;25:1–81.

34. Huang Y, Datta A, Bikson M, Parra LC. Realistic volumetric-approach to simulate transcranial electric stimulation—ROAST—a fully automated open-source pipeline. *J Neural Eng*. 2019;16(5):056006.
35. Saturnino GB, Puonti O, Nielsen JD, Antonenko D, Madsen KHH, Thielscher A. SimNIBS 2.1: a comprehensive pipeline for individualized electric field modelling for transcranial brain stimulation. *bioRxiv*. 2018;500314.
36. Opitz A, Paulus W, Will S, Antunes A, Thielscher A. Determinants of the electric field during transcranial direct current stimulation. *Neuroimage*. 2015;109:140–50.
37. Huang Y, Parra LC, Haufe S. The New York Head—a precise standardized volume conductor model for EEG source localization and tES targeting. *NeuroImage* [Internet]. 140. Available from: [internal-pdf://100.120.191.80/NeuroImage\\_\(\\_\)2015p\\_.pdf](http://www.ncbi.nlm.nih.gov/pubmed/26706450) <http://www.ncbi.nlm.nih.gov/pubmed/26706450>.
38. Windhoff M, Opitz A, Thielscher A. Electric field calculations in brain stimulation based on finite elements: an optimized processing pipeline for the generation and usage of accurate individual head models. *Hum Brain Mapp*. 2013;34:923–35.
39. Bikson M, Rahman A, Datta A. Computational models of transcranial direct current stimulation. *Clin EEG Neurosci*. 2012;43:176–83.
40. Saturnino GB, Antunes A, Thielscher A. On the importance of electrode parameters for shaping electric field patterns generated by tDCS. *Neuroimage*. 2015;120:25–35.
41. Wagner T, Eden U, Rushmore J, Russo CJ, Dipietro L, Fregni F, et al. Impact of brain tissue filtering on neurostimulation fields: a modeling study. *Neuroimage*. 2014;85(Pt 3):1048–57.
42. Gullmar D, Haueisen J, Reichenbach JR. Influence of anisotropic electrical conductivity in white matter tissue on the EEG/MEG forward and inverse solution. A high-resolution whole head simulation study. *Neuroimage*. 2010;51:145–63.
43. Opitz A, Windhoff M, Heidemann RM, Turner R, Thielscher A. How the brain tissue shapes the electric field induced by transcranial magnetic stimulation. *Neuroimage*. 2011;58:849–59.
44. Ruffini G, Fox MD, Ripolles O, Miranda PC, Pascual-Leone A. Optimization of multifocal transcranial current stimulation for weighted cortical pattern targeting from realistic modeling of electric fields. *Neuroimage*. 2014;89:216–25.
45. Kammer T, Vorwerk M, Herrmberger B. Anisotropy in the visual cortex investigated by neuro-navigated transcranial magnetic stimulation. *Neuroimage*. 2007;36:313–21.
46. Neuling T, Wagner S, Wolters CH, Zaehle T, Herrmann CS. Finite-element model predicts current density distribution for clinical applications of tDCS and tACS. *Front Psych*. 2012;3:83.
47. Miranda PC, Faria P, Hallett M. What does the ratio of injected current to electrode area tell us about current density in the brain during tDCS? *Clin Neurophysiol*. 2009;120:1183–7.
48. Salvador R, Wenger C, Miranda PC. Investigating the cortical regions involved in MEP modulation in tDCS. *Front Cell Neurosci* [Internet]. 2015;9. Available from: [internal-pdf://80.246.106.242/FrontCellNeurosci9\(\\_\)2015pp.pdf](http://www.frontiersin.org/Journal/Abstract.aspx?s=156&name=cellular_neuroscience&ART_DOI=10.3389/fncel.2015.00405) [http://www.frontiersin.org/Journal/Abstract.aspx?s=156&name=cellular\\_neuroscience&ART\\_DOI=10.3389/fncel.2015.00405](http://www.frontiersin.org/Journal/Abstract.aspx?s=156&name=cellular_neuroscience&ART_DOI=10.3389/fncel.2015.00405).
49. Datta A, Bansal V, Diaz J, Patel J, Reato D, Bikson M. Gyri-precise head model of transcranial direct current stimulation: Improved spatial focality using a ring electrode versus conventional rectangular pad. *Brain Stimul*. 2009;2:201–7.
50. Datta A, Bikson M, Fregni F. Transcranial direct current stimulation in patients with skull defects and skull plates: high-resolution computational FEM study of factors altering cortical current flow. *Neuroimage*. 2010;52:1268–78.
51. Datta A, Baker JM, Bikson M, Fridriksson J. Individualized model predicts brain current flow during transcranial direct-current stimulation treatment in responsive stroke patient. *Brain Stimul*. 2011;4:6.
52. Dmochowski JP, Datta A, Bikson M, Su YZ, Parra LC. Optimized multi-electrode stimulation increases focality and intensity at target. *J Neural Eng* [Internet]. 2011;8. Available from: [internal-pdf://0293331575/JNeuralEng8\(4\)2011p46011.pdf](http://www.ncbi.nlm.nih.gov/pubmed/22011461).
53. Jurcak V, Tsuzuki D, Dan I. 10/20, 10/10, and 10/5 systems revisited: their validity as relative head-surface-based positioning systems. *Neuroimage*. 2007;34:1600–11.
54. Laakso I, Tanaka S, Koyama S, De Santis V, Hirata A. Inter-subject variability in electric fields of motor cortical tDCS. *Brain Stimul*. 2015;8:906–13.



55. Fischer DB, Fried PJ, Ruffini G, Ripolles O, Salvador R, Banus J, et al. Multifocal tDCS targeting the resting state motor network increases cortical excitability beyond traditional tDCS targeting unilateral motor cortex. *NeuroImage*. 2017;157:34–44.
56. Radman T, Ramos RL, Brumberg JC, Bikson M. Role of cortical cell type and morphology in subthreshold and suprathreshold uniform electric field stimulation in vitro. *Brain Stimul*. 2009;2(215):28.
57. Reato D, Rahman A, Bikson M, Parra LC. Low-intensity electrical stimulation affects network dynamics by modulating population rate and spike timing. *J Neurosci*. 2010;30(45):15067–79.
58. Gerstner W, Kempter R, van Hemmen JL, Wagner H. A neuronal learning rule for sub-millisecond temporal coding. *Nature*. 1996;383(6595):76–81.
59. Modolo J, Thomas AW, Legros A. Possible mechanisms of synaptic plasticity modulation by extremely low-frequency magnetic fields. *Electromagn Biol Med*. 2013;32(2):137–44.
60. Schmidt SL, Iyengar AK, Foulser AA, Boyle MR, Fröhlich F. Endogenous cortical oscillations constrain neuromodulation by weak electric fields. *Brain Stimul*. 2014;7(6):878–89.
61. Fresnoza S, Christova M, Feil T, Gallasch E, Körner C, Zimmer U, et al. The effects of transcranial alternating current stimulation (tACS) at individual alpha peak frequency (iAPF) on motor cortex excitability in young and elderly adults. *Exp Brain Res*. 2018;236(10):2573–88.
62. Vossen A, Gross J, Thut G. Alpha power increase after transcranial alternating current stimulation at alpha frequency ( $\alpha$ -tACS) reflects plastic changes rather than entrainment. *Brain Stimul*. 2015;8(3):499–508.
63. Reato D, Rahman A, Bikson M, Parra LC. Effects of weak transcranial alternating current stimulation on brain activity—a review of known mechanisms from animal studies. *Front Hum Neurosci* [Internet]. 2013 [cited 2019 Sep 13];7. Available from: <http://journal.frontiersin.org/article/10.3389/fnhum.2013.00687/abstract>.
64. Merlet I, Birot G, Salvador R, Molaee-Ardekani B, Mekonnen A, Soria-Frish A, et al. From oscillatory transcranial current stimulation to scalp eeg changes: a biophysical and physiological modeling study. *PLoS One* [Internet]. 2013.; Available from: <http://www.scopus.com/inward/record.url?eid=2-s2.0-84874530177&partnerID=MN8TOARS>.
65. Coombes S. Waves, bumps, and patterns in neural field theories. *Biol Cybern*. 2005;93(2):91–108.
66. Hodgkin AL, Huxley AF. A quantitative description of membrane current and its application to conduction and excitation in nerve. *Bull Math Biol*. 1990;52(1–2):25–71.
67. Wilson HR, Cowan JD. Excitatory and Inhibitory interactions in localized populations of model neurons. *Biophys J*. 1972;12(1):1–24.
68. Breakspear M. Dynamic models of large-scale brain activity. *Nat Neurosci*. 2017;20(3):340–52.
69. Hagmann P, Kurrant M, Gigandet X, Thiran P, Wedeen VJ, Meuli R, et al. Mapping human whole-brain structural networks with diffusion MRI. *PLoS One*. 2007;2(7):e597.
70. Bassett DS, Bullmore ET. Human brain networks in health and disease. *Curr Opin Neurol*. 2009;22(4):340–7.
71. Feldt S, Bonifazi P, Cossart R. Dissecting functional connectivity of neuronal microcircuits: experimental and theoretical insights. *Trends Neurosci*. 2011;34(5):225–36.
72. Bassett DS, Sporns O. Network neuroscience. *Nat Neurosci*. 2017;20(3):353–64.
73. Sanchez-Todo R, Salvador R, Santarnecchi E, Wendling F, Deco G, Ruffini G. Personalization of hybrid brain models from neuroimaging and electrophysiology data. *BioRxiv*. 2018.
74. Ruffini G. Application of the reciprocity theorem to EEG inversion and optimization of EEG-driven transcranial current stimulation (tCS, including tDCS, tACS, tRNS). *arXiv*. 2015;29(2013):1–11.
75. Molaee-Ardekani B, Márquez-Ruiz J, Merlet I, Leal-Campanario R, Gruart A, Sánchez-Campusano R, et al. Effects of transcranial Direct Current Stimulation (tDCS) on cortical activity: a computational modeling study. *Brain Stimul*. 2013;6:25–39.
76. Lefaucheur J-P, Wendling F. Mechanisms of action of tDCS: a brief and practical overview. / [data/revues/09877053/unassign/S0987705319301790/](https://www.em-consulte.com/en/article/1306771) [Internet]. 2019 24 [cited 2019 Oct 1]; Available from: <https://www.em-consulte.com/en/article/1306771>.

77. Liang Z, Duan X, Su C, Voss L, Sleight J, Li X. A pharmacokinetics-neural mass model (PK-NMM) for the simulation of EEG activity during propofol anesthesia. *PLoS One*. 2015;10(12):1–21.
78. Kurbatova P, Wendling F, Kaminska A, Rosati A, Nabbout R, Guerrini R, et al. Dynamic changes of depolarizing GABA in a computational model of epileptogenic brain: insight for Dravet syndrome. *Exp Neurol*. 2016;283(Pt A):57–72.
79. Goldenberg MM. Overview of drugs used for epilepsy and seizures. *P T*. 2010;35(7):392–415.
80. Dayan P, Abbott LF. *Theoretical neuroscience: computational and mathematical modeling of neural systems*. Cambridge: The MIT Press; 2005.
81. Bansal K, Nakuci J, Muldoon SF. Personalized brain network models for assessing structure-function relationships. *Curr Opin Neurobiol*. 2018;52:42–7.
82. Aerts H, Fias W, Caeyenberghs K, Marinazzo D. Brain networks under attack: robustness properties and the impact of lesions. *Brain*. 2016;139(Pt 12):3063–83.
83. Cabral J, Luchhoo H, Woolrich M, Joensson M, Mohseni H, Baker A, et al. Exploring mechanisms of spontaneous functional connectivity in MEG: how delayed network interactions lead to structured amplitude envelopes of band-pass filtered oscillations. *Neuroimage*. 2014;90:423–35.
84. Marchitelli R, Aiello M, Cachia A, Quarantelli M, Cavaliere C, Postiglione A, et al. Simultaneous resting-state FDG-PET/fMRI in Alzheimer disease: relationship between glucose metabolism and intrinsic activity. *Neuroimage*. 2018;176:246–58.
85. Villemagne VL, Doré V, Burnham SC, Masters CL, Rowe CC. Imaging tau and amyloid- $\beta$  proteinopathies in Alzheimer disease and other conditions. *Nat Rev Neurol*. 2018;14(4):225–36.
86. Sepulcre J, Sabuncu MR, Li Q, Fakhri GE, Sperling R, Johnson KA. Tau and amyloid  $\beta$  proteins distinctively associate to functional network changes in the aging brain. *Alzheimers Dement*. 2017;13(11):1261–9.
87. Canolty RT, Edwards E, Dalal SS, Soltani M, Nagarajan SS, Kirsch HE, et al. High gamma power is phase-locked to theta oscillations in human neocortex. *Science*. 2006;313(5793):1626–8.
88. Farzan F, Barr MS, Levinson AJ, Chen R, Wong W, Fitzgerald PB, et al. Evidence for gamma inhibition deficits in the dorsolateral prefrontal cortex of patients with schizophrenia. *Brain*. 2010;133(5):1505–14.